Beamforming Features of the Grounded Dielectric Substrate Based X-Band Monopole Antenna

I.V. Ivanchenko, *Senior Member, IEEE*, N.A. Popenko, *Senior Member, IEEE,*
M.M. Khruslov, *Student Member, IEEE,* R.E. Chernobrovkin, *Student Member, IEEE*

Abstract – **Computational modelling of the cylindrical monopole antenna with the grounded dielectric layer is carried out. Notice that the near-field distributions in the inductive region of the given class of antennas are similar to the spatial periodical lattice with different number of variations along the ground radius and with the amplitude decrease to the antenna edge. The calculated antenna characteristics are validated by measurements on the antenna prototypes. The basic regularities of the radiation pattern formation are analyzed.**

Index Terms – **field; monopole antenna; antenna measurement; antenna radiation pattern**

I. Introduction

The growing demand of wireless services requires the definition of new standards providing an increased degree of mobility for the end-user and a higher speed of the data transmission. Among emerging standards, one of the most promising is the *IEEE 802.16 (WiMax 2GHz<f<60GHz*) able to support high-speed wireless broadband applications with rather long reach, mobility, and roaming [1, 2]. With these remarks in mind, a problem of the antenna miniaturization becomes a topical question. In this respect there is a necessity of carrying out the special investigations to take correctly into account the diffraction effects. Currently, there are many publications focusing an attention on the effect of ground plane dimensions [3, 4, 5, 6, 7]. In particular, as regards the monopole antenna operating at *f=2GHz* it has been shown that the elevation angle of the peak directivity depends essentially on the ground plane size [4]. From the numerical and experimental results with respect to the different X-band monopole antenna designs the authors of the papers [5, 6, 7] show a contribution of EM fields scattered from the ground plane edges on the antenna beamforming.

The monopole antenna partially or entirely buried in the grounded dielectric substrate seems to be a one of the challenging designs for achieving the desired radiation characteristics at the relatively small antenna dimensions. In such a way, the characteristics of monopole antenna in the dielectric layer with the soft and hard boundary conditions of the vertical *E* field are analyzed depending on the dielectric and magnetic permittivity [8]. The soft surface is realized by either corrugations or different material loadings whereas a smooth conducting disk gives a hard boundary condition. It has been found a possibility to prevent the wave from propagating along the surface and thereby reduce the edge diffraction effects. Along with that, by using the modal expansion method the input impedance and radiation power of the monopole antenna depending on the monopole environment permittivity, dielectric layer thickness and monopole height were learned in [9]. Nevertheless, the problem of the ground plane effect on the radiation pattern formation in antennas of this kind needs the further investigations.

This paper is devoted to the comprehensive investigations of the X-band cylindrical monopole antenna with the grounded dielectric layer with the aim to determine the basic regularities of antenna beamforming taking into account the grounded dielectric substrate dimensions and the layer permittivity.

II. Antenna Design

Antenna under testing (AUT) is the cylindrical monopole being composed of the coaxial central core located over the circular ground plane. The monopole is buried in the dielectric layer with permittivity ε_r (Fig. 1). The monopole height is d_{1r} and the radius of both the ground plane and the dielectric layer is R. It should be noted that in all the cases the monopole height amounts to the height of dielectric layer.

Manuscript received October 27, 2008.
Igor Ivanchenko is with the Usikov Institute for Radiophysics and Electronics of the National Academy of Sciences of Ukraine, 12 Ak. Proskura St., Kharkov, 61085, Ukraine, tel. +38 (057) 7203594, fax. +38 (057) 3152105 (e-mail: ireburan@yahoo.com).
Nina Popenko is with the Usikov Institute for Radiophysics and Electronics of the National Academy of Sciences of Ukraine, 12 Ak. Proskura St., Kharkov, 61085, Ukraine, tel. +38 (057) 7203594, fax. +38 (057) 3152105 (e-mail: ireburan@yahoo.com).
Khruslov M.M. is with the Usikov Institute for Radiophysics and Electronics of the National Academy of Sciences of Ukraine, 12 Ak. Proskura St., Kharkov, 61085, Ukraine, tel. +38 (057) 7203594, fax. +38 (057) 3152105 (e-mail: ireburan@yahoo.com).
Chernobrovkin R.E. is with the Usikov Institute for Radiophysics and Electronics of the National Academy of Sciences of Ukraine, 12 Ak. Proskura St., Kharkov, 61085, Ukraine, tel. +38 (057) 7203594, fax. +38 (057) 3152105 (e-mail: ireburan@yahoo.com).

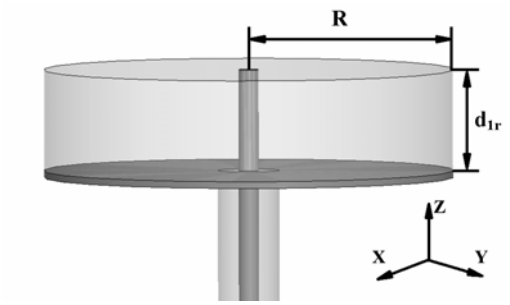

Fig.1. Geometry of the antenna with monopole embedded in the dielectric layer

III. METHODS AND EQUIPMENT

The computational modeling of monopole antennas with the dielectric layer was performed by means of the special software developed earlier [5, 7]. In experiments we have carried out the investigations of EM field distributions in the inductive and far-field regions of the AUT. When measuring the near-field distributions in the inductive region, we used the special probes and methods described in [10].

Radiation pattern measurements were performed in the fast sweep frequency mode of the SHF oscillator with the discrete of 10MHz in the every point of the receiving horn antenna position. At that, the angular discrete of the horn position is 0.5^0. This technique developed by us earlier [11] is very convenient and allows analyzing quickly the radiation characteristics of the AUT over the entire operational frequency band.

IV. RESULTS AND DISCUSSION

Numerical simulations of antenna characteristics were performed for different grounded substrate radii (7,5mm≤R≤110mm) and the layer permittivity ε_r=2,3; 2,5; 3,16; 4,67; 6,84; 9,65; 12. Our preliminary investigations have shown [5] that the radiation characteristics of the cylindrical monopole antenna could be weakly modified in case the monopole height is changed in the limits of $d_{1r}=\lambda/4$=7.5mm ±5mm, (here and hereinafter λ=30mm), namely: S_{11} (±0,5dB), bandwidth (±50MHz), whereas the resonance frequency remains the same. As a result, the quarter-wave cylindrical monopole (d_{1r}=7,5mm at the frequency f=10GHz) has been chosen in this study.

Below the radiation pattern behavior, the distribution of the current density |J|(x,y,z) on the ground plane surface, the input reflection coefficient, as well as the antenna bandwidth and gain are analyzed in the frequency band 6GHz - 12GHz.

V. MONOPOLE ANTENNAS WITH DIFFERENT GROUND RADII

The simulated results have shown that the input reflection coefficient S_{11} of antennas with the relative layer permittivity ε_r=2.5 and radii 7.5mm<R<15mm is higher than -10dB. With the ground plane radius increase from R=15mm to R=110mm a number of resonances in the operational frequency band increases from the one to the seven (Fig. 2).

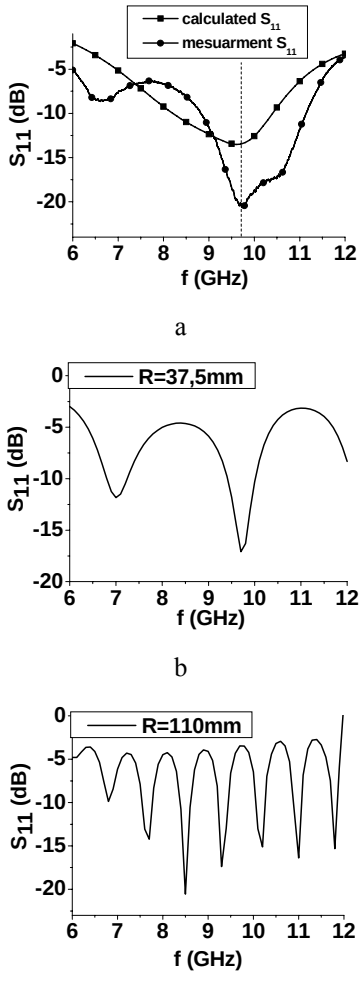

Fig. 2. Input reflection coefficient of monopole antennas with the grounded dielectric substrate: (a) R=15mm, (b) R=37.5mm, (c) R=110mm

As one sees from the Fig. 2a one has a single resonance for the antenna with R=15mm over the entire operational frequency band. With the radius increase up to R=22.5mm this resonance is shifted towards the higher frequencies. When the grounded substrate radius of antenna is changed within the limits 30mm<R<40mm, the two resonances appear in the analyzed frequency band (Fig. 2b). The subsequent radius increase up to R=110mm leads to an increase in the number of resonances, namely: we can observe a one resonance for R=15mm, the two resonances for R=37.5mm, the three resonances for R=60mm, and the seven resonances for R=110mm (Fig. 2c). Such the feature of AUT properties seems to be useful in designing the multi-band antennas. However, in this case the radiation pattern shape should be the same at the every resonance frequency of antenna.

The numerical results were validated by means of measurements performed on the Agilent Network Analyzer PNA-L N5230A. A good correlation between the calculated

and measured values of the resonance frequencies and the antenna bandwidth has been shown (Fig. 2a). Some discrepancy in the S_{11} behavior is attributed to the fact that the layer permittivity in calculations and in the experiment can differ.

The investigations of near-fields in the inductive region of antennas with the relative layer permittivity ε_r=2.5 were carried out to make clear a nature of these resonances. As an example, the current density |J|(x,y,z) on the ground plane surface of the three antenna prototypes with R_1=15mm, R_2=37.5mm, and R_3=110mm for a one of resonances excited in the given antennas are shown in the Fig. 3 and Fig. 4. Since the well-defined the current density |J|(x,y,z) on the ground plane surface corresponds to the every resonance frequency one may pronounce that the resonant modes are exited in this kind of antennas. In this way, the current density |J|(x,y,z) on the ground plane surface of antennas with R≤15mm is described by the Gauss like function (Fig.3a). It is worth noting that the simulated distributions are in good agreement with the experimental ones measured at a standoff distance of 2mm from the antenna surface (Fig. 4a). At the same time, for antennas with the radii R>30mm the resonant modes are excited as a result of the spatial filtration of partial waves reflected from the grounded substrate edges (Fig.2b, c). In this case the EM field distribution corresponding to the every resonance mode is the interference picture as the spatial periodical lattice with a different number of variations along the ground plane radius and with the amplitude decrease to the antenna edge (Fig.3b, c). In particular, the three field variations are observed along the ground radius at a one of resonant modes for the antenna with R=37,5mm (Fig.3b and Fig.4b), whereas a number of variations amounts to the eight for the antenna with R=110mm (Fig. 3c). It should also be noted that the similar near-field distributions are observed in the inductive region of the dielectric disk antennas [12].

From this study it has been determined that for antennas with the ground radii R>37.5mm a set of resonant modes is excited with the different spatial configuration. For the fixed R a number of EM field variations along the ground radius in the inductive region increases per unit at the transition from the one resonant mode to the next one towards the higher frequency.

The analysis of calculated radiation patterns in the frequency band allows analyzing a dynamics of the radiation pattern shape transformation with the frequency increase (Fig.5). As one sees from the Fig. 5a, the antenna with R=15mm produces mono-beam radiation pattern which remains virtually the same over the entire analyzed frequency band. At the same time, the antenna with R=37.5mm produces two-beam radiation pattern at the resonance frequency f_1=7.0GHz, whereas at the frequency f_2=9.75GHz the radiation pattern has already five lobes (Fig. 5b). As regards the antenna with R=110mm the radiation pattern in the analyzed frequency band split to a number N_F of lobes, namely: f_1=6.7GHz, N_F=9; f_2=7.6GHz, N_F=11; f_3=8.45GHz, N_F=13; f_4=9.28GHz, N_F=14; f_5=10.17GHz, N_F=15; f_6=11.0GHz, N_F=17; f_7=11.83GHz, N_F=17 (Fig. 5c).

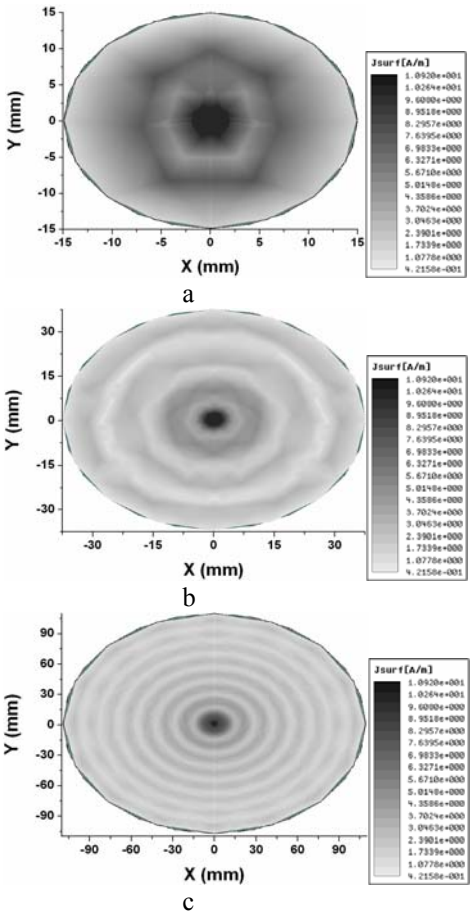

Fig. 3. Simulated the current density |J|(x,y,z) on the ground plane surface of the monopole antenna for different ground radii: (a) R=15mm, f=9.57GHz; (b) R=37.5GHz, f=8.93GHz; (c) R=110mm, f=8.51GHz. White and black colors correspond to the minimum and maximum of the current density |J|(x, y) on the ground surface, respectively

Let consider, for example, the radiation pattern transformation for the antenna with R=60mm in more detail. It can be seen that the different radiation pattern shape is observed at the every resonance frequency (Fig. 6). In particular, the antenna produces five-lobe radiation pattern at f_1=8.1GHz (Fig. 6a). A number of side lobes increases up to seven ones at f_2=9.3GHz (Fig. 6b). Finally, the radiation pattern is transformed into eight-lobe picture at the highest resonance frequency f_3=11.2GHz (Fig. 6c).

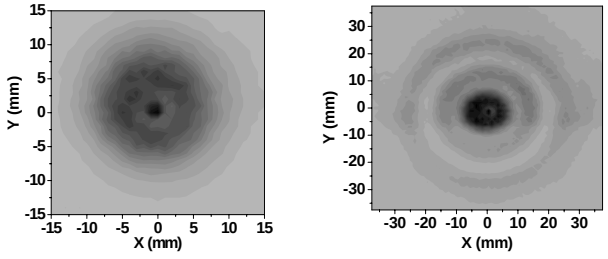

Fig. 4. Measured near-field distribution in the inductive region of antennas (a) R=15mm, f=9.57GHz; (b) R=37.5GHz, f=8.93GHz. White and black colors correspond to the minimum and maximum of the H_φ-component, respectively

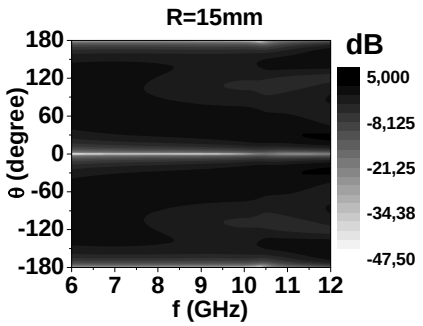

a

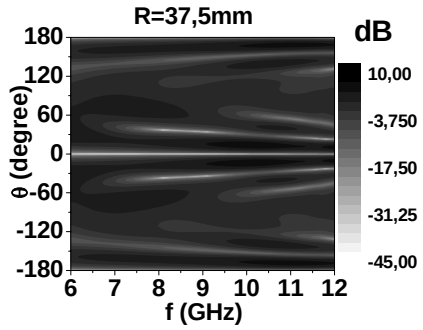

b

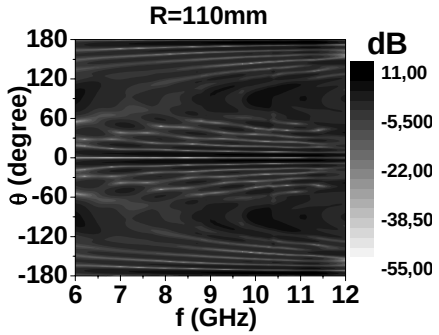

c

Fig. 5. Radiation patterns of monopole antennas for different radii: white and black colors correspond to the minimum and maximum directivity, respectively

Thus, the behavior of radiation pattern transformation of antennas with ground radii R>37.5mm allows determining their general properties, namely: (i) at all the resonance frequencies we observe the lobe near zenith; (ii) the radiation power in the azimuth plane is virtually the same; (iii) for antennas with any constant R a number of lobes in the radiation pattern increases moving towards the higher resonant modes.

With these remarks in mind the use of such the antennas as the multi-band ones seems to be impossible owing to the fact that the radiation patterns differ.

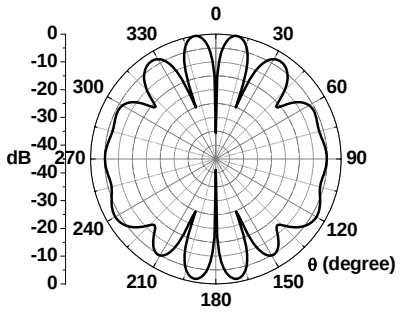

a

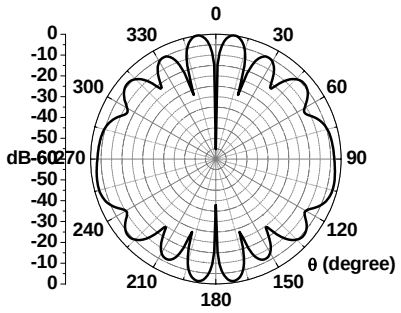

b

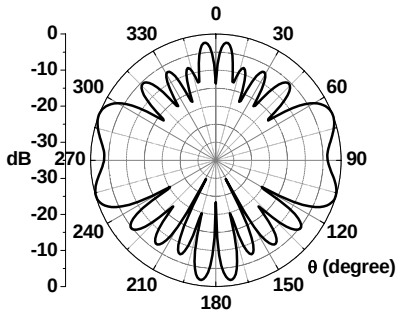

c

Fig. 6. Radiation patterns of monopole antennas (R=60mm, ε_r=2.5) for different resonant modes: (a) f=8.1GHz, (b) f=9.3GHz, (c) f=11.2GHz

As can be seen from the Fig. 7a, the experimental radiation pattern is in a good agreement with the simulated one for the antenna with R=15mm. However, for the antennas with multi-beam radiation pattern (for example, for the antenna with R=60mm) there is a qualitative similarity bearing in mind a number of lobes and their location in the space (Fig. 7b). At that the visible discrepancy in the radiation power can be attributed to the distinctions in the complex constants of dielectric materials used in the simulations and in the experiment.

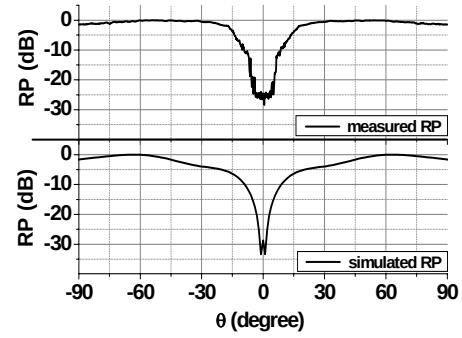

a

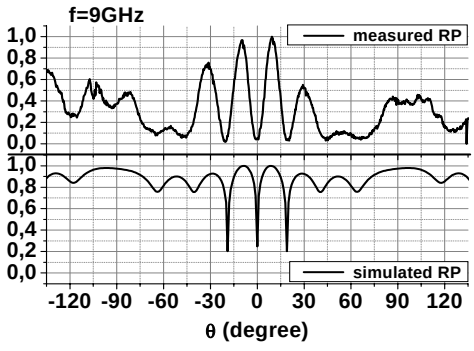

b

Fig. 7. Calculated and measured radiation patterns of monopole antennas (a) R=15mm, f=9.7GHz; (b) R=60mm, f=9.0GHz

It should also be noted that the monopole antenna with the grounded substrate can operate at higher frequencies too (f=35GHz - 39GHz). In fact, by means of the usual scaling transformation, the antenna with parameters d_{1r}=2mm and R=4mm is chosen to operate in the long-wave region of millimeter range. The simulated input reflection coefficient and radiation pattern have shown that the given antenna is the extremely wideband one allowing to produce the wide beamwidth in the azimuth plane (Fig. 8). However, the operational frequency band of antenna prototype is sufficiently narrow (Δf=36.4-37.08GHz) (Fig. 8a). At the same time the calculated and measured radiation patterns at the resonance frequency f=36.7GHz completely coincide (Fig. 8b).

VI. MONOPOLE ANTENNAS WITH DIFFERENT LAYER PERMITTIVITY

The layer permittivity is the evident parameter allowing one to control the antenna performance. For aforementioned antenna designs we have performed the simulations of the input reflection coefficient and radiation patterns for different dielectric layer permittivity. In particular, for antennas with R≤15mm the resonance shifting is observed towards the higher frequencies with the layer permittivity increase. It has been found that the characteristic feature of these dependencies is an availability of the optimal layer permittivity providing the maximum bandwidth (Δf=2.3GHz, ε_r=2.5) or maximum antenna gain (G=3.8, ε_r=3.7) (Fig. 9). Based on the dependencies depicted in the plot one may design the antennas with bandwidth and gain given in advance.

For antennas with R≥30mm the layer permittivity increase results in increasing a number of resonant modes as well as reducing the operational frequency band (Table 1).

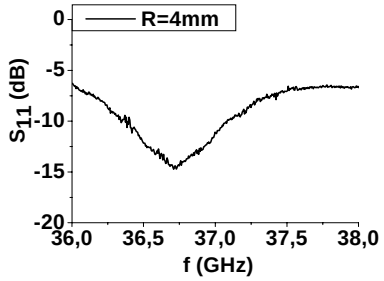

a

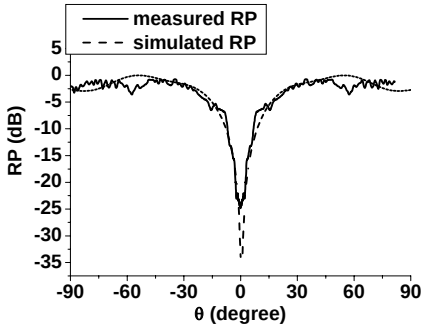

b

Fig. 8. (a) Measured input reflection coefficient; (b) calculated and measured radiation patterns of the monopole antenna (R=4mm, ε_r=2.5, f=37.2GHz)

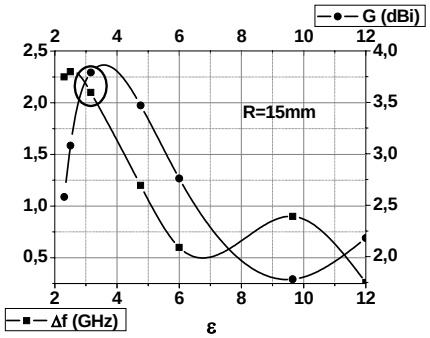

Fig. 9. Simulated gain and bandwidth of the monopole antenna versus the layer permittivity (R=15mm)

TABLE 1
AUT CHARACTERISTICS

	R=15mm			R=22.5mm			R=30mm			R=60mm		
ε_r	f_r, GHz	Δf, GHz	N_F	f_r, GHz	Δf, GHz	N_F	f_r, GHz	Δf, GHz	N_F	f_r, GHz	Δf, GHz	N_F
2.3	9.8	8.3-10.55	1	11.2	10,9-11,6	3	8.6	8,15-9,1	3	8.3	8,1-8,57	5
										10	9,81-10,18	6
										11.6	11,45-11,73	7
2.5	9.5	8-10.3	1	10.9	10,45-11,28	3	8.4	7,91-8,79	3	8.1	7,86-8,29	5
							11.3	11,38-11,89	3	9.3	9,48-9,86	7
										11.2	11,06-11,36	10
3.16	8.4	7.4-9.41	1	9.9	9,52-10,26	3	7.7	7,31-7,99	2	7.4	7,2-7,54	5
							10.6	10,32-10,84	4	8.7	8,58-8,89	7
										10.1	9,93-10,21	7
										11.4	11,26-11,48	8
4.76	6.9	6.35-7.55	1	8.3	8,11-8,45	2	6.4	6,26-6,57	1	6.2	6,14-6,29	3
							8.8	8,61-8,94	3	7.3	7,26-7,32	5
							11.0	10,91-11,04	3	8.4	8,33-8,42	6
										9.4	9,34-9,52	7
										10.5	10,24-10,56	7

VII. ANTENNA FOR WIMAX APPLICATIONS

Aforementioned results allow designing the compact antennas with mono-beam radiation pattern and the elevation angle of peak directivity near the azimuth plane. Based on the results highlighted in Fig. 9 the relative layer permittivity ε_r=3.16 for the monopole antenna with the ground radius R=15mm has been selected and the antenna prototype has been manufactured. As one sees from the Fig. 10a the agreement between theory and experiment is quite good. This antenna produces mono-beam radiation pattern in the wide frequency band (Δf=2.1GHz, Fig. 10a) with the elevation angle of peak directivity $\theta_{max}=59^0$ (Fig. 10b).

VIII. CONCLUSION

Comprehensive investigations of the cylindrical monopole antenna in the dielectric layer have been carried out in the frequency range 6GHz<f<12GHz. The antenna characteristics have been analyzed depending on the ground radius and the layer permittivity. By using the near-field technology it has been found that the EM field distributions in the inductive region at the resonance frequencies are similar to the spatial periodical lattice with a different number of variations along the ground radius with the general low of the field power decrease to the antenna edge For antennas with R>30mm the spatial field distribution of excited modes has been determined for the suitable pair of R and ε_r. It has been found that for the fixed ground radius and layer permittivity the radiation pattern is transformed at the transition from the one resonant mode to the next one with changing a number of lobes per unit.

Based on the aforementioned results, all the AUT can be sorted coming from a number of lobes N_F in the radiation pattern:

N_F=1 for the ground radii R≤15mm,

N_F=1 or N_F=3 for the radii 15<R≤30mm depending on the resonance frequency,

N_F=3 and more for the radii R>30mm.

It has been shown that for antennas with R≤15mm the permittivity increase results in the resonance frequency shift towards the higher frequencies. Notice that the mono-beam radiation pattern keeps the same within the antenna bandwidth. For antennas with R>15mm, the permittivity increase leads to increasing a number of resonant modes. In this case the multi-beam radiation pattern is produced by the antenna at the each resonance frequency.

Following the results of investigations the antenna with parameters R=15mm and ε_r=3.16 is able to shape the mono-

beam radiation pattern with the elevation angle of the peak directivity $\theta_{max}=59^0$, beamwidth $\Delta\theta=77^0$, G=3,08, Δf=24%, and resonance frequency f=8,49GHz has been presented. This monopole antenna could be widely adopted in the state-of-the-art backbone links such, for example, as *WiMax* standards-based technology.

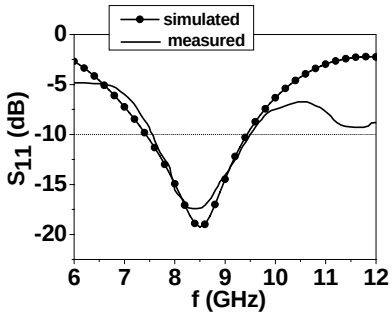

a

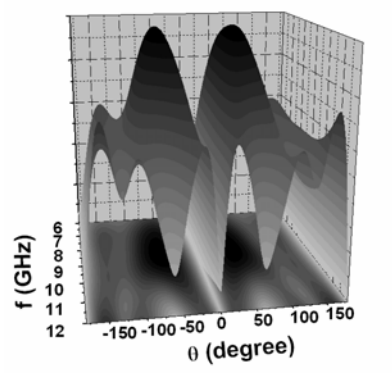

b

Fig. 10. (a) Input reflection coefficient; (b) radiation pattern of the monopole antenna (R=15mm, ε_r=3.16)

REFERENCES

[1] T.H. Kim, D.C. Park, CPW-fed compact monopole antenna for dual-band WLAN applications, Electron Lett, 41 (2005), 291-293.

[2] K.L. Wong, W.C. Su and F.S. Chang, Wideband internal folded planar monopole antenna for UMTS/WiMAX folder-type mobile phone, Microwave Optical Technol Lett, 48 (2006), 324-327.

[3] A.K. Skrivervik, J.-F. Zurcher, O. Staub, J.R. Mosig, PCS antenna design: The challenge of miniaturization, IEEE Antennas and Propagation Magazine, 43 (2001), 12–26.

[4] M.J. Ammann, Z.N. Chen, A wide-band shorted planar monopole with bevel, IEEE Antennas and Propagation Magazine, 51 (2003), 901.

[5] I.V. Ivanchenko, A.M. Korolev, V.L. Pazynin, N.A. Popenko, M.M. Khruslov, The features of radiation pattern formation of the monopole antenna with finite screens. Telecommunications and Radioengineering, 65 (2006), 1859-1869.

[6] I.V. Ivanchenko, A.M. Korolev, V.L. Pazynin, N.A. Popenko, M.M. Khruslov Effect of finite screen and monopole's height on radiation characteristics of monopole antenna, In: Proc MICON-2006, 729-731.

[7] M.M. Khruslov, V. Pazynin, X-band coaxial monopole antenna with an additional metal screen, Journal of Telecommunications and Information Technology, 1 (2007), 30-34.

[8] Zhinong Ying, Per-Simon Kildal, , and Ahmed A. Kishk, Study of Different Realizations and Calculati Models for Soft Surfaces by Using a Vertic Monopole on a Soft Disk as a Test, IEEE Trans Antennas Propag, 44 (1996), 1474-1481.

[9] S. Zhongxiang, H. Robert, Modeling of a Monopole Partially Buried in a Grounded Dielectric Substrate by the Modal Expansion Method. IEEE Trans Antennas Propag, 44 (1996), 1535-1536.

[10] I.V. Ivanchenko, D.I. Ivanchenko, A.M. Korolev, N.A. Popenko, Experimental studies of X-band leaky-wave antenna performances, Microwave and optical technology letters, 35 (2002), 277-281.

[11] A.S. Andrenko, I.V. Ivanchenko, D.I. Ivanchenko,. S.Yu. Karelin, A.M. Korolev, E.P. Laz'ko, and N.A. Popenko, Active Broad X-Band Circular Patch Antenna. IEEE Antennas Wireless Propag Lett, 5 (2006), 529-533.

[12] A. Andrenko, I. Ivanchenko, N. Popenko, M. Khruslov, Near-field characterization and radiation properties of circular dielectric patch antennas, In: Proc ICONIC (2005), 174-179.

Igor Ivanchenko was born in Kharkov, Ukraine, in 1952. In June 1975 he graduated from the Kharkov State University and received the MS degree in Radiophysics. From 1975 to the present he works at the Institute for Radiophysics & Electronics of the National Academy of Sciences of Ukraine (IRE NASU). He received the Ph.D and D.Sc. degrees in Radiophysics in 1980 and 1997, respectively. From 1984 he is a Senior Researcher with the Department of Radio-Spectroscopy in the IRE NASU. He has authored and co-authored more than 100 publications in the fields of electromagnetics, non-destructive testing, low-temperature magnetic radio-spectroscopy, and semiconductor physics. Currently he is a Head of the Laboratory of High Frequency Technology at IRE NASU. Prof. I.Ivanchenko is a Senior Member of IEEE and a Member of EuMa.

Nina Popenko was born in Gadyach, Ukraine, in 1948. In June 1971 she graduated from the Kharkov Institute of Radioelectronics and received the MS degree in Radio-technique. From 1971 to the present she works at the Usikov Institute for Radiophysics and Electronics of the National Academy of Sciences of Ukraine (IRE NASU). She received the Ph.D and D.Sc. degrees in Radiophysics in 1981 and 1998, respectively. From 2007 she is a Leading Researcher with the Department of Radio-Spectroscopy in the IRE NASU. She has authored and co-authored more than 120 publications in the fields of low-temperature magnetic radio-spectroscopy, semiconductor physics, and antennas design. Prof. N. Popenko is a Senior Member of IEEE, and a Member of EuMa.

Maksym Khruslov was born in Kharkov, Ukraine, in 1982. He received the M.S. degree in radiophysics and electronics from Karazin Kharkov National University (Ukraine) in 2004. Since 2004, he works in the Institute for Radiophysics and Electronics of the National Academy of Sciences of Ukraine, Kharkov, Ukraine, where he is currently as Junior Researcher with the Radiospectroscopy Department. His research interest includes the near-field technology, computational modeling of microwave antennas. Mr. Maksym Khruslov is a Student Member of IEEE, and a Member of EuMa.

Roman Chernobrovkin was born in Kharkov, Ukraine, in 1983. He received the M.S. degree in radiophysics and electronics from Karazin Kharkov National University (Ukraine) in 2005. Since 2005, he works in the Institute for Radiophysics and Electronics of the National Academy of Sciences of Ukraine, Kharkov, Ukraine, where he is currently as Junior Researcher with the Radiospectroscopy Department. His research interest includes computational modeling of microwave antennas and the phased antenna arrays. Roman Chernobrovkin is a Student Member of IEEE, and a Member of EuMa.